IMPROVED PREDICTIONS OF LOW AND MODERATE DRAG REDUCTION IN TURBULENT CHANNEL FLOW OF FENE-P FLUIDS USING k-ε MODEL

P. R. Resende

Centro de Estudos de Fenómenos de Transporte, Universidade do Porto, Portugal

F. T. Pinho

Centro de Estudos de Fenómenos de Transporte, Universidade do Porto, Portugal

K. Kim

Dep. Mechanical Engineering, Hanbat National University, Daejeon, South Korea

R. Sureshkumar

Dep. Energy, Environmental and Chemical Engineering, Washington University of St. Louis, St Louis, MO, USA

B. A. Younis

Dep. Civil and Environmental Engineering, University of California, Davis, USA

IVth Workshop on Research in Turbulence and Transition

ERCOFTAC Iberian West PC Partners Meeting - 16th October 2009
Lisbon, Portugal

Motivation and DNS cases: channel flow of FENE-P

Objective: modifications to existing k-ε model + performance

Pinho, Li, Younis & Sureshkumar JNNFM 154 (2008) 89
A low Reynolds number turbulence closure for viscoelastic fluids

RANS model

Turbulence modeling: Step 1) a priori DNS closure development
Step 2) building closures into the model

Fully-developed channel flow

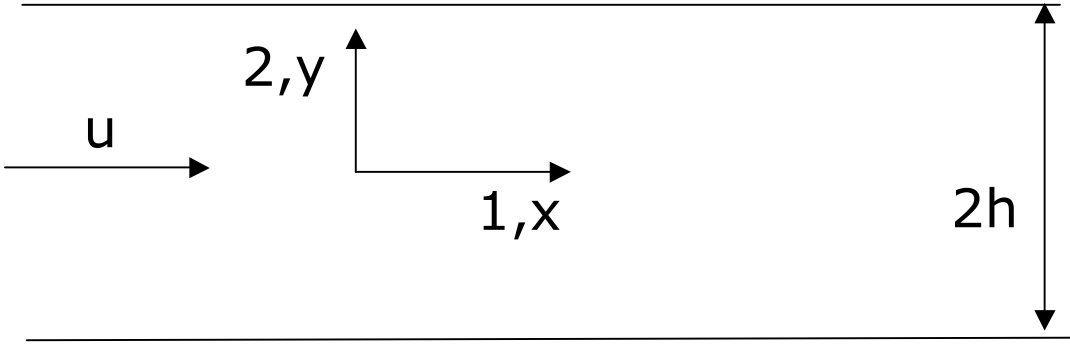

$$We_\tau = \frac{\lambda u_\tau^2}{\nu_0}$$

$$Re_\tau = \frac{h u_\tau}{\nu_0}$$

DNS test/calibration cases (FENE-P model)

$$Re_\tau = 395, \beta = 0.9, L^2 = 900$$

Low Drag Reduction

$$We_\tau = 25, DR = 18\%$$

High Drag Reduction

$$We_\tau = 100, DR = 37\%$$

Model of Pinho et al (2008) and New model: Governing Eqs.

Continuity: $\frac{\partial U_i}{\partial x_i} = 0$

Reynolds decomposition: $\hat{B} = B + b'$

Overbar & upper-case: time-averaged quantities

Lower-case: fluctuating quantities

Momentum balance:

$$\rho \frac{\partial U_i}{\partial t} + \rho U_k \frac{\partial U_i}{\partial x_k} = -\frac{\partial \bar{p}}{\partial x_i} + \eta_s \frac{\partial^2 U_i}{\partial x_k \partial x_k} - \frac{\partial}{\partial x_k}\left(\overline{\rho u_i u_k}\right) + \frac{\partial \bar{\tau}_{ik,p}}{\partial x_k}$$

$$\bar{\tau}_{ij} = 2\eta_s S_{ij} + \bar{\tau}_{ij,p}$$

Rheological constitutive equation: **FENE-P**

$$\bar{\tau}_{ij,p} = \frac{\eta_p}{\lambda}\left[f(C_{kk})C_{ij} - f(L)\delta_{ij}\right] + \frac{\eta_p}{\lambda}\overline{f\left(C_{kk}+c_{kk}\right)c_{ij}}$$

RACE $\rightarrow$ $\overset{\nabla}{C}_{ij} + \overline{u_k \frac{\partial c_{ij}}{\partial x_k}} - \left(\overline{c_{kj}\frac{\partial u_i}{\partial x_k}} + \overline{c_{ik}\frac{\partial u_j}{\partial x_k}}\right) = -\frac{\bar{\tau}_{ij,p}}{\eta_p}$

M_{ij} CT_{ij} NLT_{ij}

Closures required

$$f\left(\hat{C}_{kk}\right) = \frac{L^2 - 3}{L^2 - \hat{C}_{kk}}$$

Conformation (RACE) equation

$$\lambda \overset{\nabla}{C}_{ij} + \lambda \left[\cancel{u_k \frac{\partial c_{ij}}{\partial x_k}} - \left(\overline{c_{kj} \frac{\partial u_i}{\partial x_k}} + \overline{c_{ik} \frac{\partial u_j}{\partial x_k}} \right) \right] = -\left[f(C_{kk}) C_{ij} - f(L)\delta_{ij} \right] - \cancel{\overline{f(C_{kk}) c_{ij}}}$$

M_{ij} $\quad$ CT_{ij} $\quad$ NLT_{ij}

Pinho et al, JNNFM 154 (2008) 89

$$f(C_{mm}) \frac{NLT_{ij}}{\lambda} = f_{\mu_1} \left[\frac{C_{E_3} u_\tau^2}{\nu_0^2} C_{kk} \overline{u_i u_j} + \frac{C_{\alpha_{14}}}{\nu_0} \left(\overline{u_i u_k} W_{kn} C_{nj} + \overline{u_j u_k} W_{kn} C_{ni} + \overline{u_k u_i} W_{jn} C_{nk} \right) \right]$$

New model (based on exact equation)

$$f(C_{mm}) \frac{NLT_{ij}}{\lambda} = \frac{f(C_{mm})}{\lambda} \left\{ f_{N_1} C_{ij} \frac{f(C_{mm})}{\lambda} - f_{N_2} \left[C_{kj} \frac{\partial U_i}{\partial x_k} + C_{ik} \frac{\partial U_j}{\partial x_k} \right] \right\}$$

$$+ f_{N_3} \left[\frac{C_{kn}}{\nu_0 \sqrt{2 S_{pq} S_{pq}}} \left[\overline{u_i u_m} \frac{\partial U_j}{\partial x_k} \frac{\partial U_m}{\partial x_n} + \overline{u_j u_m} \frac{\partial U_i}{\partial x_k} \frac{\partial U_m}{\partial x_n} \right] + \frac{1}{\nu_0 \sqrt{2 S_{pq} S_{pq}}} \left[\frac{\partial U_k}{\partial x_n} \frac{\partial U_m}{\partial x_k} \left(C_{jn} \overline{u_i u_m} + C_{in} \overline{u_j u_m} \right) \right] \right]$$

$$- f_{N_4} \left[C_{jn} \frac{\partial U_k}{\partial x_n} \frac{\partial U_i}{\partial x_k} + C_{in} \frac{\partial U_k}{\partial x_n} \frac{\partial U_j}{\partial x_k} + C_{kn} \left(\frac{\partial U_j}{\partial x_n} \frac{\partial U_i}{\partial x_k} + \frac{\partial U_i}{\partial x_n} \frac{\partial U_j}{\partial x_k} \right) \right] + f_{N_5} \frac{4}{15} \frac{\varepsilon^N}{\beta \left(\nu_s + \nu_{\tau_p} \right)} C_{mm} \delta_{ij}$$

$$f_{N_i} = f(We_{\tau_0}, y^+) \quad \text{(only two depend on } y^+\text{)}$$

Reynolds stress model: eddy viscosity model

Prandtl-Kolmogorov model (k-ε closure)

$$-\overline{u_i u_j} = 2\nu_T S_{ij} - \frac{2}{3} k\delta_{ij}$$

Pinho et al, JNNFM 154 (2008) 89

$$\nu_T = C_\mu f_\mu \frac{k^2}{\tilde{\varepsilon}^N + \varepsilon^V}$$

Viscoelastic stress work

Dissipation of k by solvent

New model

$$\nu_T = \nu_T^N - \nu_T^P$$

$$\nu_T^N = C_\mu f_\mu \frac{k^2}{\tilde{\varepsilon}^N}$$

$$\nu_T^P = C_\mu^P f_\mu^P C_{kk} \frac{k^2}{\tilde{\varepsilon}^N}$$

$$\frac{k^2}{\tilde{\varepsilon}^N} \propto lu'$$

Transport equation for k and viscoelastic stress work (ε^V)

$$\rho\frac{Dk}{Dt} = -\rho\overline{u_i u_k}\frac{\partial U_i}{\partial x_k} - \rho\overline{u_i}\frac{\overline{\partial k'}}{dx_i} - \frac{\partial\overline{p'u_i}}{\partial x_i} + \eta_s\frac{\partial^2 k}{\partial x_i\partial x_i} - \eta_s\overline{\frac{\partial u_i}{\partial x_k}\frac{\partial u_i}{\partial x_k}} + \frac{\partial\overline{\tau'_{ik,p}u_i}}{\partial x_k} - \overline{\tau'_{ik,p}}\frac{\partial u_i}{\partial x_k}$$

0 | P_k | Q^N | D^N | $-\varepsilon^N$ | Q^V | $-\varepsilon^V$

exact | unchanged | exact | Slightly changed | Changed

$$\varepsilon^V \equiv \frac{1}{\rho}\overline{\tau'_{ik,p}\frac{\partial u_i}{\partial x_k}} \approx \frac{\eta_p}{\rho\lambda}\left[\overline{c_{ik}f\left(C_{mm}+c_{mm}\right)\frac{\partial u_i}{\partial x_k}}\right]$$

$$\overline{f'c'_{ik}\frac{\partial u_i}{\partial x_k}} \approx f_{\varepsilon^V}\times f\left(C_{mm}\right)\overline{c_{ik}\frac{\partial u_i}{\partial x_k}}$$

$f_{\varepsilon^V} = f_{\varepsilon^V}(We)$

NLT_{ii}

Model is the same, except for NLT_{ii} and corrective $f_{\varepsilon}{}^{V}$

$$0 = \frac{d}{dy}\left[\left(\eta_s + \frac{\rho f_T \nu_T}{\sigma_k}\right)\frac{dk}{dy}\right] + P_k - \rho\tilde{\varepsilon}^N - \rho D^N + \frac{\eta_p}{\lambda}\frac{d}{dy}\left[f\left(C_{mm}\right)\frac{C_{nk}\left(FU\right)_n + CU_{nny}}{2}\right] - \eta_p\frac{f\left(C_{mm}\right)}{\lambda}\frac{NLT_{nn}}{2}$$

Transport equation for ε^N

Exact equation: not used, this equation is completely modeled

$$2\nu_s \overline{\frac{\partial u_i}{\partial x_m}\frac{\partial}{\partial x_m}\left(\rho\frac{Du_i}{Dt}\right)} + 2\nu_s \overline{\frac{\partial u_i}{\partial x_m}\frac{\partial}{\partial x_m}\left(\rho u_k\frac{\partial U_i}{\partial x_k}\right)} + 2\nu_s \overline{\frac{\partial u_i}{\partial x_m}\frac{\partial}{\partial x_m}\left(\rho\frac{\partial u_i u_k}{\partial x_k}\right)}$$

$$+2\nu_s \overline{\frac{\partial u_i}{\partial x_m}\frac{\partial}{\partial x_m}\left(\frac{\partial p'}{\partial x_i}\right)} - 2\rho\nu_s^2 \overline{\frac{\partial u_i}{\partial x_m}\frac{\partial}{\partial x_m}\left(\frac{\partial^2 u_i}{\partial x_k^2}\right)} - 2\nu_s \overline{\frac{\partial u_i}{\partial x_m}\frac{\partial}{\partial x_m}\left(\frac{\partial \tau'_{ik,p}}{\partial x_k}\right)} = 0$$

Polymer modifies ε^N equation
(neglected by Pinho et al, JNNFM 154 (2008) 89
but considered in new model)

- Need to reduce ε^N as polymer drag reduction increases
- Extra term should be a destruction term, like the classical destruction term, i.e., proportional to ε^2/k

Transport model equation for ε^N

Pinho et al, JNNFM 154(2008) 89

$$0 = \frac{d}{dy}\left[\left(\eta_s + \frac{\rho f_T \nu_T}{\sigma_\varepsilon}\right)\frac{d\tilde{\varepsilon}^N}{dy}\right] + \rho f_1 C_{\varepsilon_1}\frac{\tilde{\varepsilon}^N}{k}\frac{P_k}{\rho} - \rho f_2 C_{\varepsilon_2}\frac{\varepsilon^{N^2}}{k} + \rho E + E_{\tau_p}$$

Destruction term

with $E_{\tau_p} = 0$

Low *Re* correction
Nagano & Hishida, JFE 109 (1987) 156

New model

$E_{\tau_p} \neq 0$

Modeled as as extra destruction related to polymer extension and viscoelastic stress work

$$E_{\tau_p} = -\left\{f_{E_{\tau p1}}\varepsilon^V + f_{E_{\tau p2}}\left[C_{nn} f\left(C_{ii}\right)\right]^2 \varepsilon^N\right\}\frac{\tilde{\varepsilon}^N}{k} \propto \frac{\varepsilon \times \varepsilon^N}{k} \sim \frac{u'^4}{l^2}$$

$$f_{E_{\tau p1}}, f_{E_{\tau p2}} = f_{E_{\tau p}}\left(We, y^+\right)$$

Reference cases 1: $Re_{\tau 0}$= 395; β=0.9, L^2=900

Mean velocity

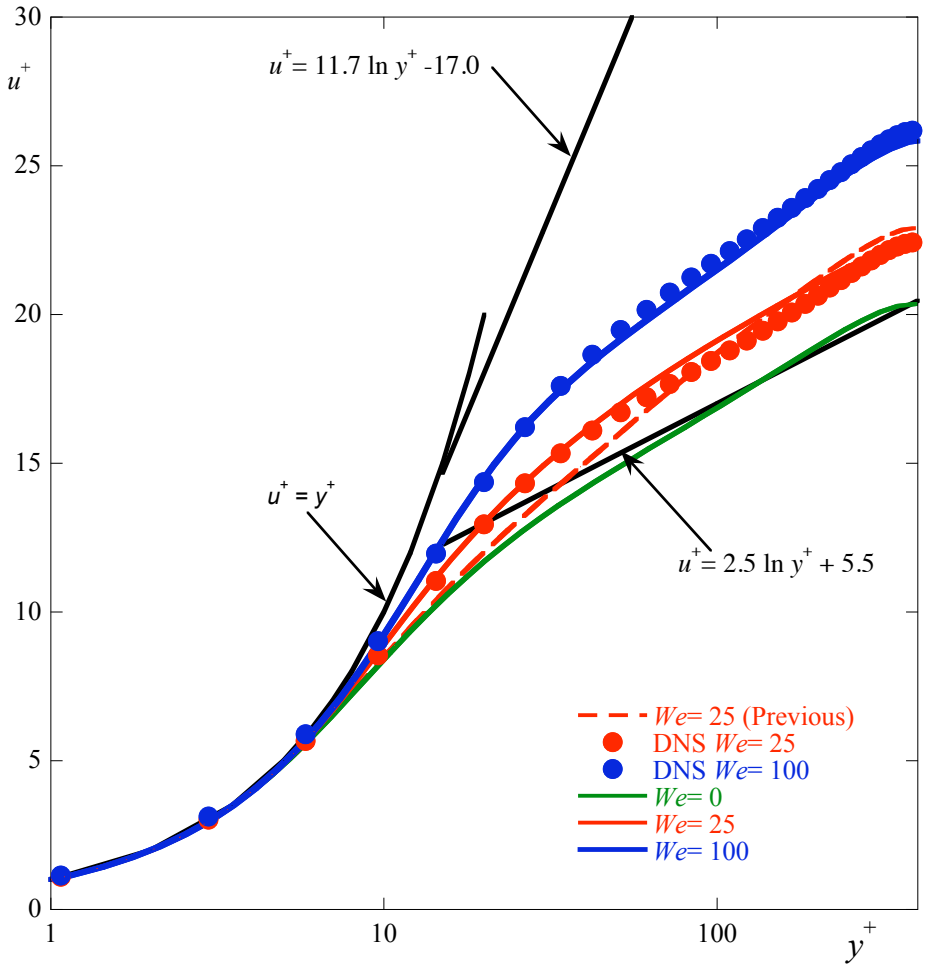

k^+

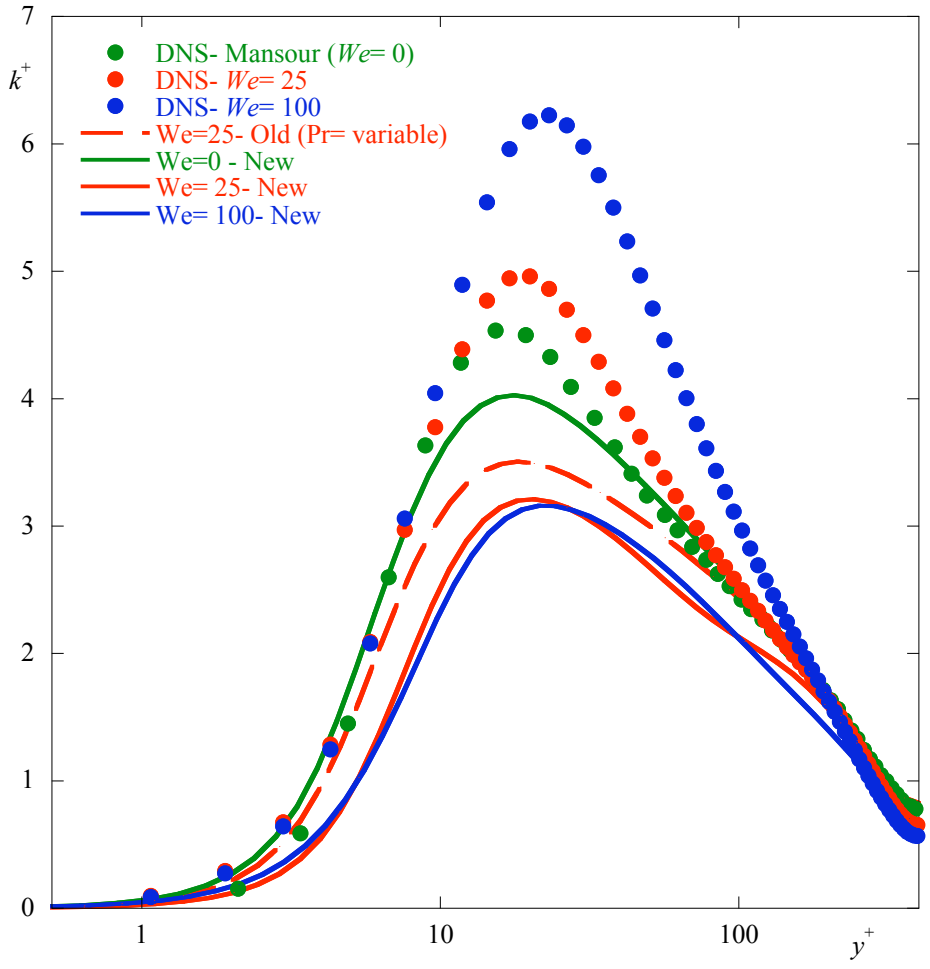

Reference cases 2: $Re_{\tau 0}$= 395; β=0.9, L^2=900

ε^{N+}

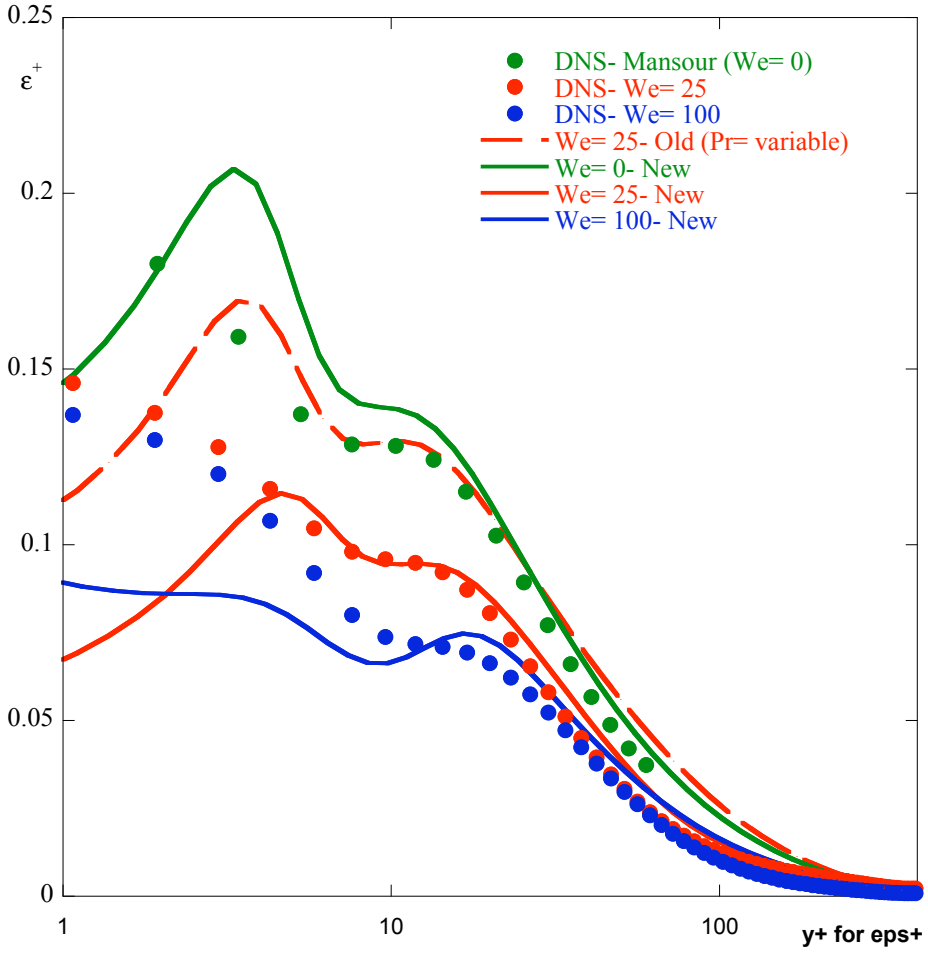

NLT^{*}_{ii}

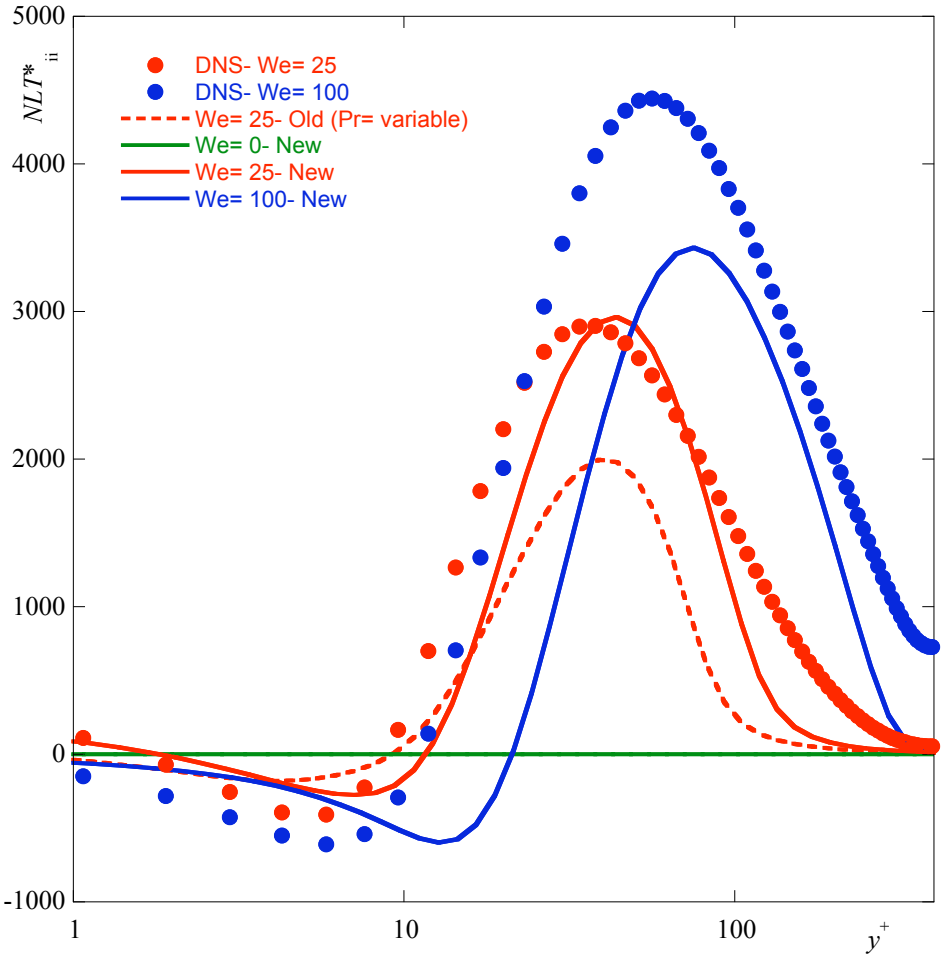

Reference cases 3: $Re_{\tau 0}$= 395; β=0.9, L^2=900

$\overline{u'v'}^{+}$

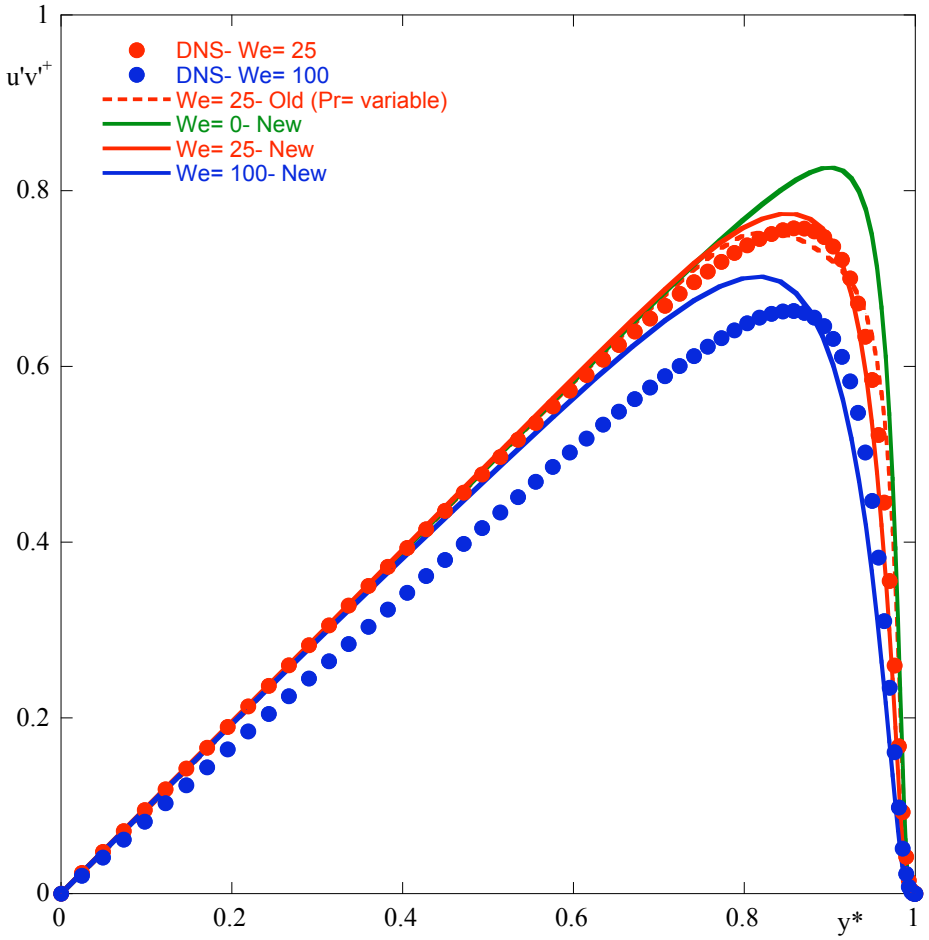

$\overline{\tau}^{+}_{xy,p}$

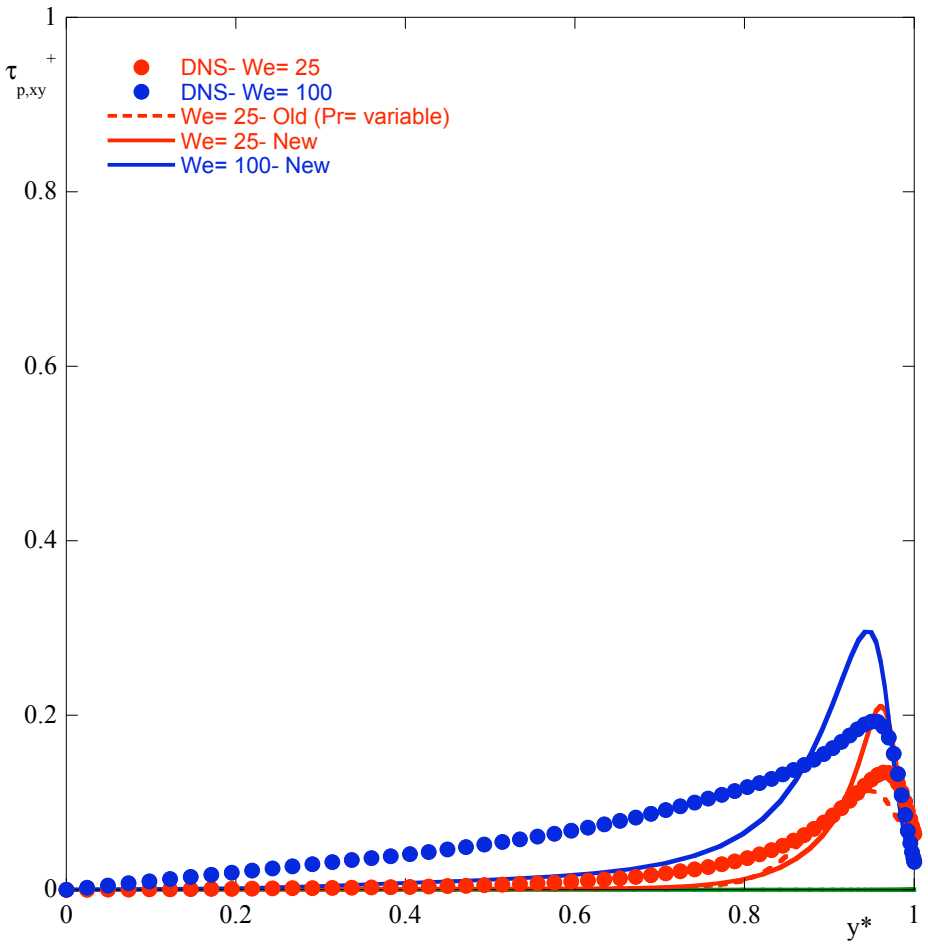

Parametric study 1: $Re_{\tau 0}$= 395; β=0.9, L^2=900

Mean velocity

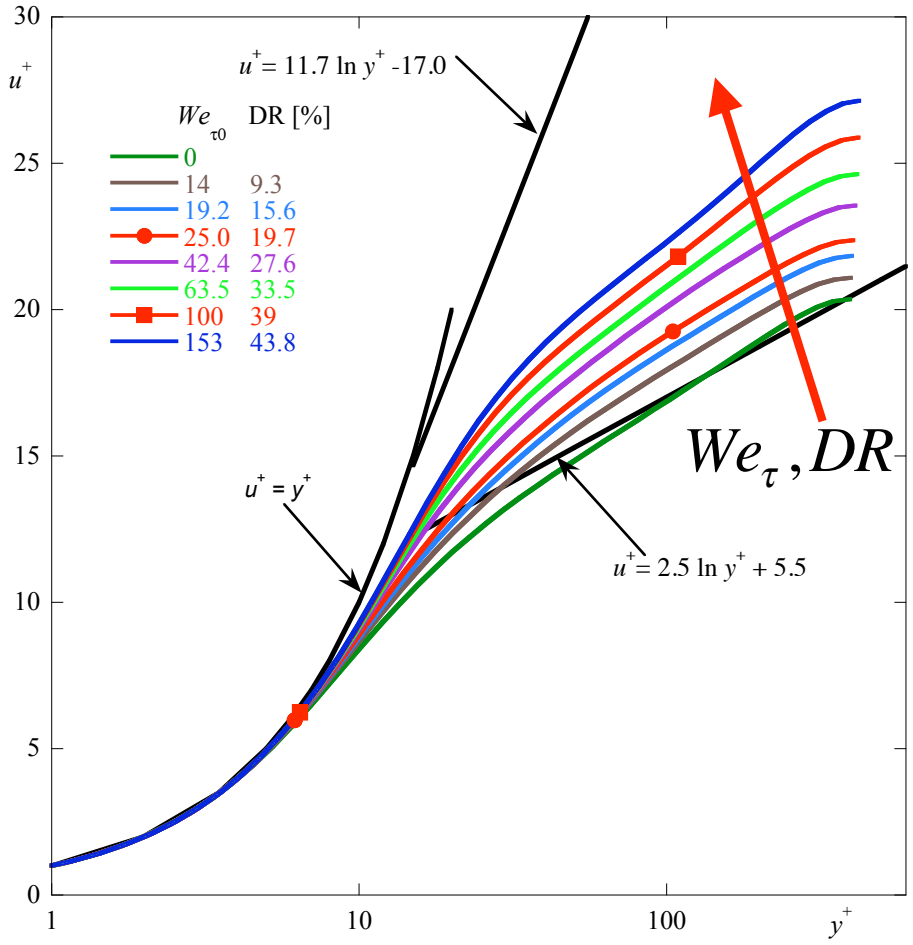

k^+

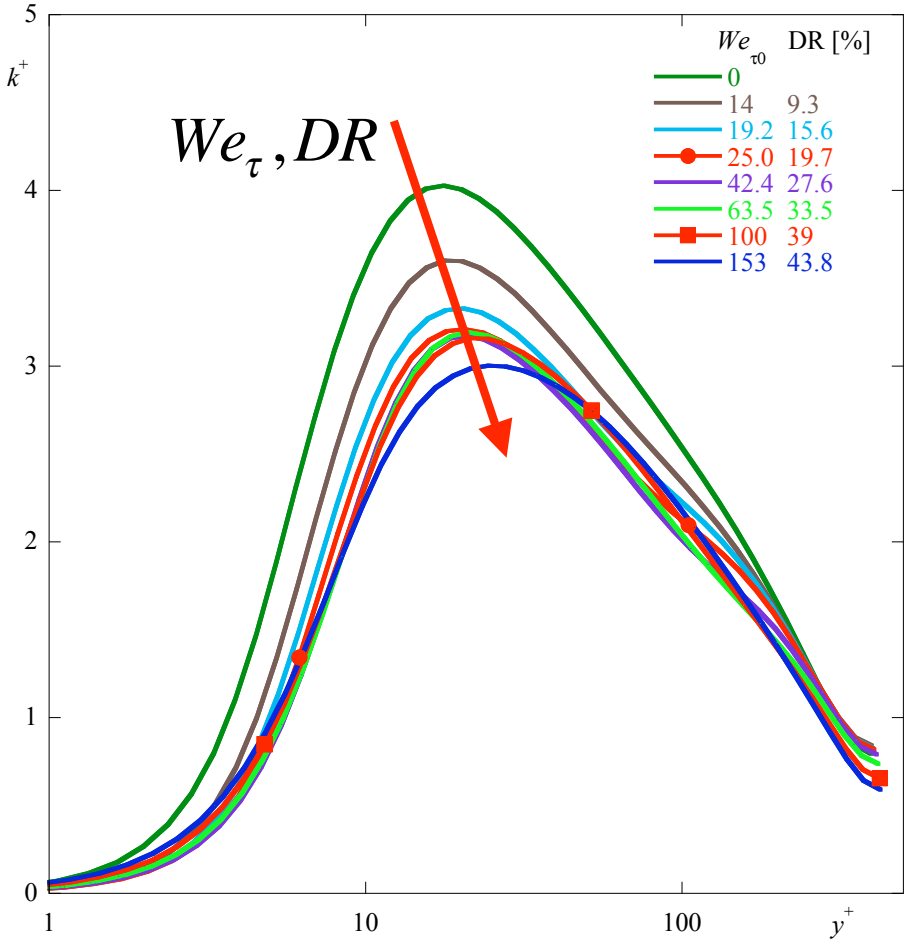

Parametric study 2: $Re_{\tau 0}$= 395; β=0.9, L^2=900

ε^{N+}

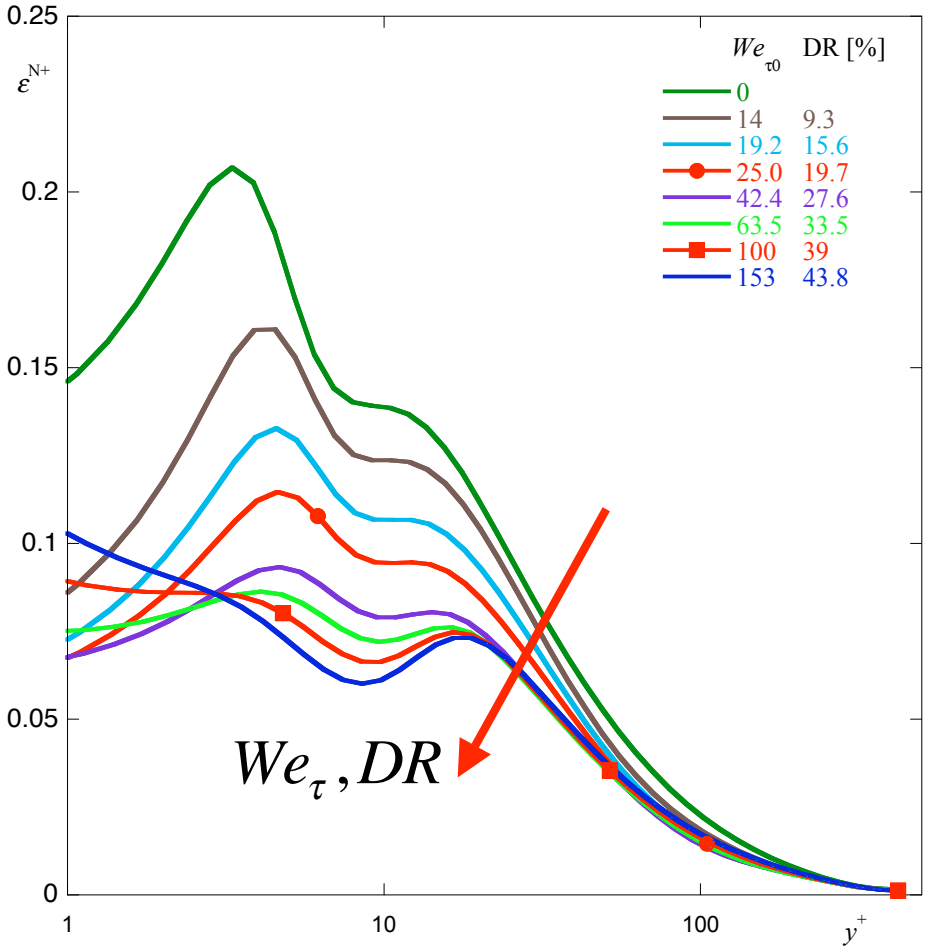

NLT^*_{ii}

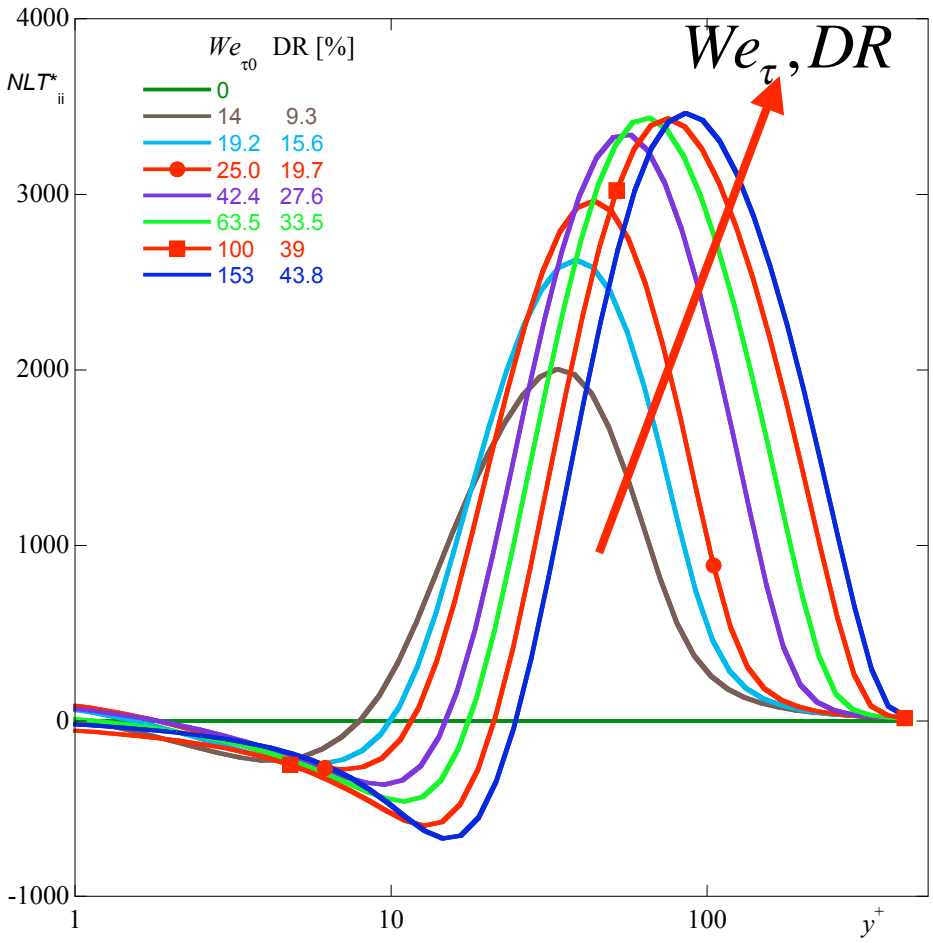

Parametric study 3: $Re_{\tau 0}$= 395; β=0.9, L^2=900

$\overline{u'v'}^{+}$

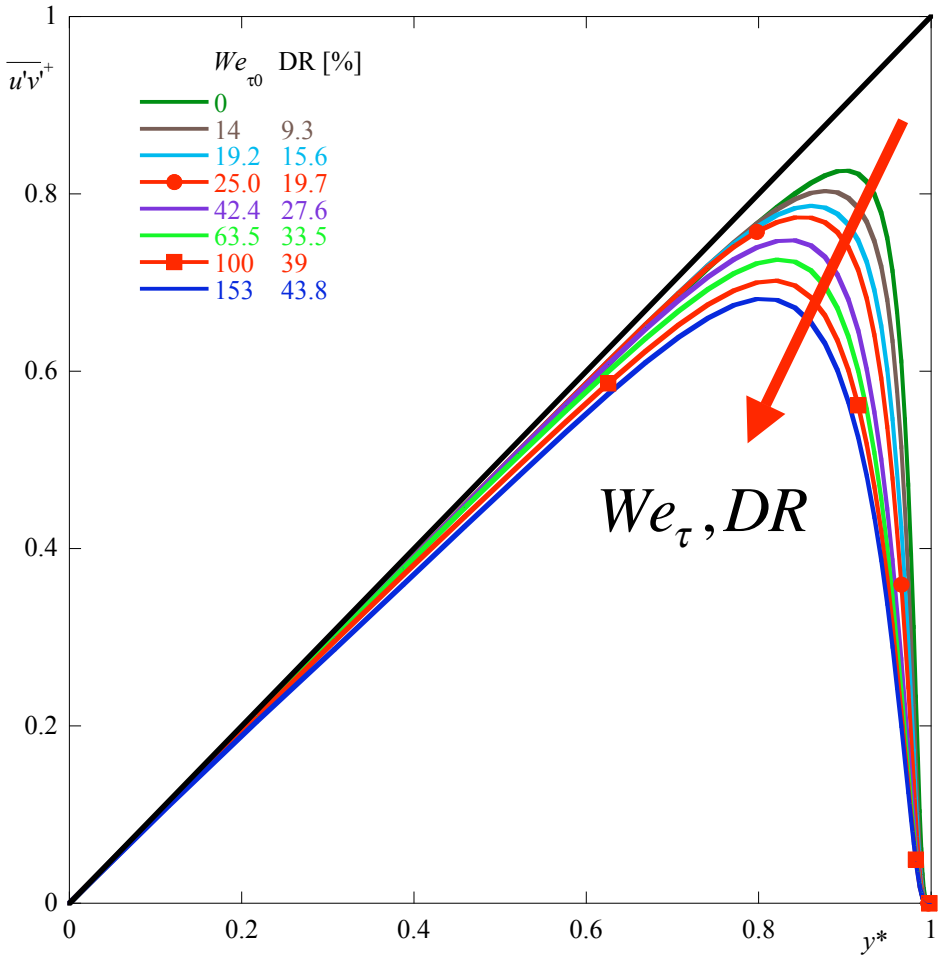

$\overline{\tau}^{+}_{xy,p}$

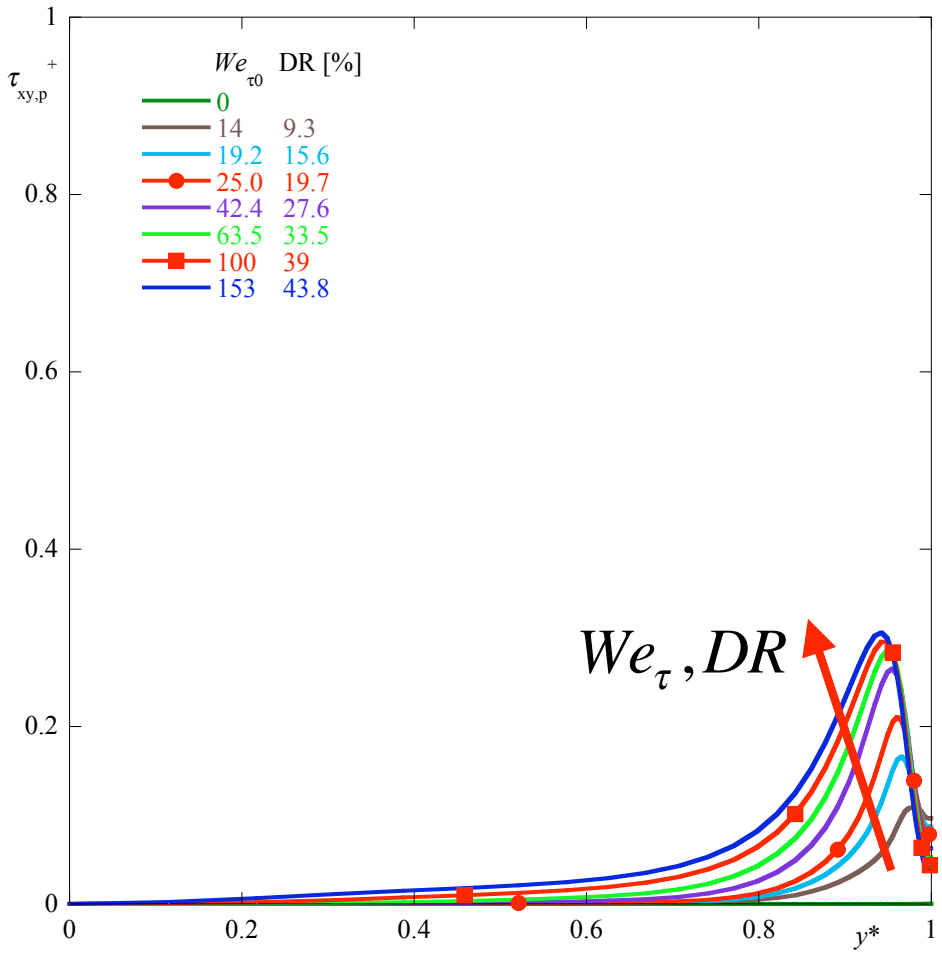

Conclusions, Future Work and Acknowledgments

- Closure for elastic contribution to ν_T
- Closure for elastic term ($E_{\tau p}$) in ε^N equation: destruction of ε^N
- k-ε model works well at Low DR and High DR (45%)

- Need to extend models to Maximum DR, & β & L^2
- To solve the existing deficiencies:

  improve k, improve polymer and Reynolds stress predictions

Acknowledgments - Funding
Fundação para a Ciência e Tecnologia
FCT Scholarship SFRH/BD/18475/2004
FCT Projects POCI/EQU/56342/2004 & PPCDT/EME/59338/2004

FOURTH WORKSHOP ON RESEARCH IN TURBULENCE AND TRANSITION

Instituto Superior Técnico
Technical University of Lisbon
Lisbon, October 16th, 2009

Iberian-West ERCOFTAC Pilot Centre

Foreword

These pages are collected summaries of communications presented at the Fourth Workshop on Research in Turbulence and Transition, held at Instituto Superior Técnico, in Lisbon on October 16th, 2009. The first edition of this Workshop was held on February 6, 2003 at the International Centre for Numerical Methods in Engineering at the Technical University of Catalonia, the second was held at the School of Aeronautical Engineering at the Technical University Madrid on February 12 of 2004, and the third one took place in the College of Engineering at the University of Seville on October 17, 2008.

These Workshops have been conducted at the initiative of CIMNE, Iberian-East and Iberian-West Pilot Centres of the European Research Community on Flow, Turbulence and Combustion (ERCOFTAC), and is a Europe-wide organization that promotes research on topics related to fluid dynamics, turbulence and combustion, and their industrial applications. More information can be found at www.ercoftac.org

The aim of this Workshop is to contribute to a better knowledge of the activities carried out by various Iberian research groups in any field relevant to the turbulence or/and Transition. The papers presented correspond to groups from Madrid, Barcelona, Seville, Zaragoza, Tarragona, Girona, Lisbon, OPorto, Coimbra, and Beira Interior.

The organizers of the Workshop want to thank the IDMEC at Instituto Superior Técnico, Technical University of Lisbon.

The Organizing Committee

Vassilis Theofilis	School of Aeronautics, Universidad Politécnica de Madrid
Roberto Castilla	Universidad Politécnica de Catalunya - Barcelona
Carlos B. da Silva	IDMEC/Instituto Superior Técnico - Lisbon

09:30	Welcome
09:40	**On the birth of stall cells on airfoils** D. Rodriguez and V. Theofilis
10:00	**Interaction between turbulence and thermal radiation in large eddy simulations of isotropic turbulent flows** M. Roger, P.J. Coelho, C.B. da Silva
10:20	**An improved k-e low Reynolds number model for low to high drag reductions in turbulent channel flow of FENE-P fluids** F. T. Pinho, P. R. Resende, K. Kim, R. Sureshkumar and B. A Younis
10:40	Coffe break
11:00	**Lag-modeling of subgrid dissipation in LES** Sergei. G. Chumakov
11:20	**Velocity and temperature evolution in PCB enclosure model** S. Varela1, G. Usera, A. Vernet and J.A. Ferré
11:40	**Stratified and Rotating Decaying Quasi-2D Flows** A. Matulka, J. A. Carrillo, L.S. Valvo and J. M. Redondo
12:00	Coffe break
12:20	**Turbulent entrainment in jets: large and small scale physics and consequences for LES** Carlos B. da Silva, Ricardo Reis, Rodrigo Taveira and J.C.F. Pereira
12:40	**Vorticity, Kinetic Energy and Momentum Analysis Of the Collision Zone between a Plane Wall Jet and a Boundary Layer** Jorge M. M. Barata, Ricardo B. F. Nunes, Pedro J.C.T. Santos and André R. R. Silva
13:00	**Symmetry breaking, intermittent transition and swirl switching in a flow of physiological interest** Joao M. M. Sousa
13:20	Lunch
15:20	**DNS simulation of a transition laminar separation bubble on a flat plate** C. Laurent, I. Mary, V. Gleize, A. Lerat, D. Arnal
15:40	**Kinetic energy and dissipation profiles calculated from RDT near a turbulent-non-turbulent interface** Miguel A. C. Teixeira and Carlos. B. da Silva
16:00	**Vortices and Spiral Features in the Ocean Surface** A. Matulka, P. Fraunie, P. Forget, J. M. Redondo, A. Platonov, M. Diez, C. Mosso, R. Castilla and E. Sekula
16:20	Coffe break
16:40	**Estimation of turbulent convection velocities and corrections to Taylor's approximation** J. C. del Álamo and J. Jiménez
17:00	**Mixing Through Stable and Unstable density interfaces** P. Lopez Gzlez-Nieto, J.L. Cano, D.Hernandez, J. M. Redondo and P. Furmanek
17:20	**Numerical Simulation of the turbulent flow in the suction chamber of an external gear pump including cavitation effects** D. Del Campo, R. Castilla and E. Codina
17:40	**Multi-fractal, Turbulent-like percolantion models in hydraulics** Diogo Bolster, Pilar Lopez Gonzalez-Nieto and Anna Tarquis
18:00	Final discussion and Conclusions
18:30	Break
20:30	Dinner at 'O Forcado'

On the birth of stall cells on airfoils

By D. Rodríguez † and V. Theofilis†

†*School of Aeronautics, Universidad Politécnica de Madrid, Pza. Cardenal Cisneros 3, E-28040 Madrid, Spain*

dani@torroja.dmt.upm.es

Global instability analyses of massively separated flow around a NACA0015 airfoil show the presence of a stationary and three-dimensional eigenmode, related to the global mode encountered in laminar separation bubbles on flat-plates. This eigenmode is unstable for a finite range of spanwise wavenumbers, while the steady basic flow is stable to two-dimensional disturbances. Topological analysis of the flow field reconstructed as the linear superposition of the basic flow and the global mode indicates that the latter origins the breakdown of the recirculation region into independent separated structures. The resulting flow patterns are resemblant to the cellular structures observed experimentally, suggesting that the instability mechanism recovered here as a global mode is on the origin of the stall cells.

Keywords: Stall Cells, Flow Topology, Global Flow Instability

Extended Summary

When a plane rectangular wing is pitched up to angles of attack just beyond stall, the separated flow on the suction side is organize into three-dimensional structures known in the literatures as *stall cells*. Oil and smoke visualizations have been used in order to recover experimental evidence of these structures (Winkelmann & Barlow, 1980) and some models of the origin and characteristics have been proposed (Winkelmann, 1988; Weihs & Katz, 1983), but the physical mechanism of the three-dimensional periodic breakdown of the two-dimensional baseline flow is presently unknown.

A previous BiGlobal instability analyses (Kitsios *et al.*, 2009) of the two-dimensional, steady laminar flow around a stalled NACA0015 airfoil at $Re_c = 200$, showed the dominance of a three-dimensional stationary mode, which exhibits the same characteristics of the global mode that appears consistently in all laminar separation bubbles (Theofilis *et al.*, 2000). Figure 2 shows the streamwise velocity component of the basic flow and the streamwise velocity amplitude function of this eigenmode.

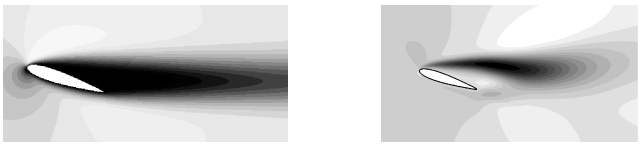

Figure 1. Left: streamwise velocity component of the basic flow; right: streamwise velocity component of the leading global mode at $\beta = 1$.

Critical-Points concepts have been employed here in order to unveil the different topological bifurcations resulting from the linear superposition of the two-dimensional basic state and the three-dimensional global mode. Special attention has been paid to the surface streamlines or skin-friction lines, in order to make direct comparisons between the present reconstructions and the experimental oil-streak topologies.

The topological description of the resulting flow is qualitatively equivalent to the stall cells recovered experimentally: spanwise periodic structures in which the separated flow regions are organized around two counter-rotating vortices, separated by fully attached bands. In addition, the periodicity length predicted by the instability analysis is in good agreement with the characteristic length observed in experiments. Comparison of the present results and stall cells in the literature suggests that the amplification of the global mode of laminar separation bubbles is a plausible origin of the stall cells (Rodríguez & Theofilis, 2009).

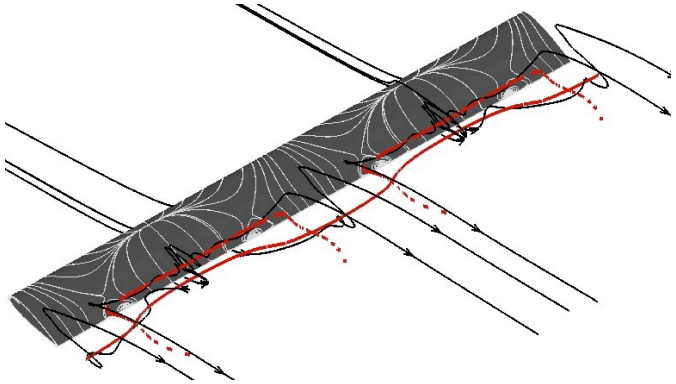

Figure 2. Cellular pattern reconstructed by linear superposition of the two-dimensional basic flow and the leading three-dimensional global mode.

The material is based upon work sponsored by the Air Force Office of Scientific Research, Air Force Material Command, USAF, under Grant number # FA8655-06-1-3066 to *nu modelling s.l.*, entitled *Global instabilities in laminar separation bubbles*. The Grant is monitored by Dr. J. D. Schmisseur of AFOSR (originally by Lt. Col. Dr. Rhett Jefferies) and Dr. S. Surampudi of EOARD. Computations have been performed on the CeSViMa (www.cesvima.upm.es), MareNostrum facilities (www.bsc.es) and DEISA-*Forschungszentrum Jülich* (www.deisa.com). The authors are grateful to Mr. V. Kitsios and Prof. J. Soria for providing the basic flow analyzed.

References

Kitsios, V., Rodríguez, D., Theofilis, V., Ooi, A. & Soria, J. 2009 Biglobal stability analysis in curvilinear coordinates of massively separated lifting bodies. *J. Comp. Phys.* **228**, 7181–7196.

Rodríguez, D. & Theofilis, V. 2009 On the birth of stall cells on airfoils. *Theor. and Comp. Fluid Dyn., to appear* .

Theofilis, V., Hein, S. & Dallmann, U. 2000 On the origins of unsteadiness and three-dimensionality in a laminar separation bubble. *Phil. Trans. Roy. Soc. London (A)* **358**, 3229–324.

Weihs, D. & Katz, J. 1983 Cellular patterns in poststall flow over unswept wings. *AIAA J.* **21**, 1757–1759.

Winkelmann, A. 1988 Separated flow on a wing at low reynolds numbers. *AIAA-88-3548* .

Winkelmann, A. & Barlow, B. 1980 Flowfield model for a rectangular planform wing beyond stall. *AIAA J.* **8**, 1006–1008.

An improved k-ε low Reynolds number model for low to high drag reductions in turbulent channel flow of FENE-P fluids

F. T. Pinho[1], P. R. Resende[1,2], K. Kim[3], R. Sureshkumar[4], B. A Younis[5]

[1]CEFT, Departamento de Engenharia Mecânica, Faculdade de Engenharia da Universidade do Porto, Rua Dr. Roberto Frias s/n, 4200 – 465 Porto, Portugal, fpinho@fe.up.pt

[2]Escola Superior de Estudos Industriais e de Gestão, Rua D. Sancho I, 981, 4480-876 Vila do Conde, Portugal resende@fe.up.pt

[3]Department of Mechanical Engineering, Hanbat National University, San 16-1, Duckmyoung-dong, Yuseong-gu, Daejeon 305-719, South Korea, kkim@hanbat.ac.kr

[4]CIM, Department of Energy, Environmental and Chemical Engineering, Washington University, St. Louis, MO 63130, U.S.A., suresh@che.wustl.edu

[5]Department of Civil and Environmental Engineering, University of California, Davis, CA 95616, USA, bayounis@ucdavis.edu

Abstract

Extensive DNS calculations of turbulent channel flow of viscoelastic fluids [1], represented by the FENE-P rheological constitutive equation, provide useful information to the development of predictive codes for industrial flows based on Reynolds-averaged equations [2]. The turbulence model of Pinho et al. [2] relied on a closure for the nonlinear term (NLT) of the Reynolds average conformation evolution equation that captured only some of its features in addition for a limited validity to low drag reduction.

Subsequent developments, presented in this work, eliminated some of the deficiencies and extended the model to high drag reduction. The new turbulence model includes a new closure for *NLT* [3], a new definition of eddy viscosity, and additional terms in the transport equations of turbulent kinetic energy and its rate of dissipation to account for the role played by the polymer stress and its fluctuations. We will present the new model, its predictions against DNS data for fully-developed channel flow, but also address existing deficiencies and outline future research needs in this area.

[1] Li C-F, Sureshkumar R and Khomami B 2006. *J. Non-Newt. Fluid Mech.*, 140, 23-40.
[2] Pinho FT, Li CF, Younis BA and Sureshkumar R 2008. *Journal of Non-Newtonian Fluid Mechanics*, 154, 89-108.
[3] Resende PR, Kim K, Pinho FT and Sureshkumar R. 2008. Paper 219_1.pdf, Proceedings of the XVth International Congress of Rheology, Monterey, California, AIP Conference Proceedings Volume 1027, Editors A. Co, L. G. Leal, R. H. Colby and A. J. Giacomin, ISBN- 978-0-7354-0550-9.

Interaction between turbulence and thermal radiation in large eddy simulations of isotropic turbulent flows.

M. Roger, P.J. Coelho and C.B. da Silva

In turbulent reactive flows, radiative heat transfer plays a significant role, and turbulence-radiation interaction (TRI) effects are relevant in most cases. This interaction between turbulence and radiation has been studied over the years, using RANS, PDF methods and more recently direct numerical simulation [1]. However, in large eddy simulation (LES), very little is known about the TRI.

In LES of thermal radiation, the subgrid-scale (SGS) radiative emission and the SGS absorption are two unclosed terms that arise after applying the filtering operation to the radiative transfer equation and which represent the effect of the SGS motions on the evolution of the resolved radiative heat flux [2]. In the present work, the influence of these SGS terms is studied.

A-priori tests based on direct numerical simulation of homogeneous isotropic turbulence have been carried out [3]. The radiative transfer equation has been solved by a ray tracing/correlated-k method. Turbulence and radiation are decoupled in the present study and combustion is not considered to simplify the analysis. The influence of the temperature variance and the spectra of the radiative terms have been analyzed.

It was found that the effect of the SGS radiative absorption may be neglected in LES, whereas the SGS radiative emission has to be modeled, particularly for engineering applications where the grids are generally coarse, and in flows with high turbulence intensities. Future works should be devoted to the development of SGS models for radiative transfer, in order to couple radiative heat transfer calculations with the numerical simulation of turbulent reactive flows.

[1] Numerical simulation of the interaction between turbulence and radiation in reactive flows, P.J. Coelho, Prog. Energy Combust. Sci. 33 (4) (2007) 311-383

[2] Analysis of the turbulence-radiation interactions for large eddy simulations of turbulent flows, M. Roger, C.B. da Silva, P.J. Coelho, Int. J. Heat Mass Transf. 52 (2009) 2243-2254

[3] Analysis of the gradient-diffusion hypothesis in large eddy simulations based on transport equations, C.B. Da Silva, J.C.F. Pereira, Phys. Fluids, 19 (035106) (2007)

Lag-modeling of subgrid dissipation in LES

Sergei G. Chumakov
Center for Turbulence Research, Stanford University
chumakov@stanford.edu

We showed recently [1] that the SGS kinetic energy $k_s = \tau_{ii}/2$ and its dissipation rate $\epsilon_s = \nu(\overline{u_{i,j}u_{i,j}} - \bar{u}_{i,j}\bar{u}_{i,j})$ generally do not scale exponentially, i.e., the relation $\epsilon_s \sim k_s^\gamma$ does not hold for a fixed γ. This exposes a flaw in a widely used model $\epsilon_s = Ck_s^{3/2}/\Delta$: contrary to the assumption of the model, the instantaneous rate of SGS energy dissipation does not have to be correlated with the instantaneous value of the SGS kinetic energy itself at the same time t. One of possible alternatives is to incorporate Lagrangian effects into modeling of the SGS dissipation, which is the aim of this work.

We describe a novel approach to modeling the dissipation rate terms that arise in one- equation LES models and in such important areas as combustion. The approach is based on using Lagrangian averaging with particular weight functions, and results in a two-equation model. The basic modeling assumption is that dissipation lags behind the production along the Lagrangian trajectory of a tracer that is carried by the resolved LES flow. The approach is applicable to modeling of both energy and scalar variance dissipation rates. The results of a priori and a posteriori tests are presented.

References

[1] S. G. Chumakov. Scaling properties of subgrid-scale energy dissipation. *Phys. Fluids*, 19:058104, 2007.

Velocity and temperature evolution in PCB enclosure model.

S. Varela[1]*, G. Usera[2], A. Vernet[1] y J.A. Ferré[1]

1: Dep. Enginyeria Mecànica.
ETSEQ, Universitat Rovira i Vigili
Av. Països Catalans 26, 43007, Tarragona, España
e-mail: {sylvanaveronica.varela, anton.vernet , josep.a.ferre}@urv.cat
web: http://ecommfit.urv.es/

2: IMFIA. Facultad de Ingeniería
Universidad de la República
J.H. Reissig 565, 1130, Montevideo, Uruguay.
e-mail: gusera@fing.edu.uy, web: http://www.fing.edu.uy/imfia/

Abstract

The main objective of this work is numerical and experimental study of velocity and temperature fields in complex domains like those encountered in computers or other electronic refrigerated systems with printed circuit board (PCB).
These PCBs are becoming smaller and therefore appear warming problems which lowers their efficiency and lifespan. The main objective is to analyze the dynamic field in order to understand it better and thus improve the effectiveness of the devices. Hence, we analyze the spatial and temporal evolution of the flow structures found in PCB enclosed cavities.
Particle Image Velocimetry (PIV) is used to obtain the experimental velocity field in a simplified model of a PCB. The numerical simulations of the velocity and temperature fields are obtained using a fully implicit finite volume method (*caffa3d.MB* [1]) that solves the 3D incompressible Navier-Stokes equations.
We work with two different geometries (Fig. 1) and two different Reynolds numbers. Analyzing PCBs enclosures models [1], shows the existence of alternate vortex shedding in the upper part of the PCB and undefined flow structure in the lower part for a low Reynolds number. A deeper knowledge of the behaviour of these structures can lead to a better enclosure design that can perform more effective heat dissipation in the PCBs.

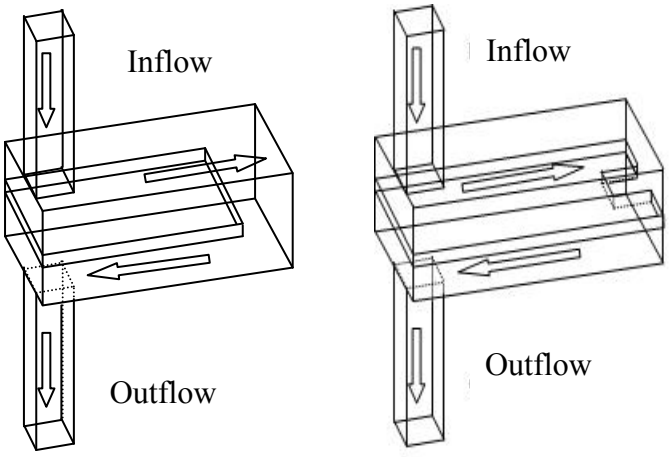

Fig 1: Domain Sketch

References

[1] G. Usera, A. Vernet, J.A. Ferré, "A Parallel Block-Structured Finite Volume Method for Flows in Complex Geometry with Sliding Interfaces", *Flow Turbulent Combust*. Vol. **81**, pp 471-495, (2008).

Stratified and Rotating Decaying Quasi-2D Flows

A. Matulka(1), J. A. Carrillo(1), L.S. Valvo (2)and J. M. Redondo(1).

(1)Dep. Fisica Aplicada, U.P.C. Campus Nord,
Barcelona 08034 Spain.
(2)Universita della Callabria. Italy

Abstract

Several sets of turbulence decaying experiments have been performed, with the aim of focusing in the middle of a strongly stratified density interface. The experiments have been done under different external conditions: a) (Non-Rotating) Decaying 2D Turbulence experiments b) Rotating Decaying 2D Turbulence experiments. And steady rotating/ stratified stirring experiments (3) Non-Rotating experiments were performed in a 1mx1m tank, while the Rotating experiments were performed in a rectangular tank of 4mx 2m; this rectangular tank was placed in the middle of the Coriolis Rotating platform from the Trondheim Marine Systems Research Infrastructure supported by the European Community TMR Project. The set of stirred experiments is a compilation of seven series of mixing experiments, dependent on the initial interfacial Richardson number. The Total time of mixing was between 53 and 72 minutes and PIV was used to map the velocity and vorticity plots in time. The density of the brine used in the experiments to create a sharp density interface was between 1007 and 1037kg m^{-3}.

The boundary conditions for all the rotating experiment are related to initial Reynolds Rer, Rossby Ro, Ekman Ek and Richardson gradient Rig numbers, the results are summarized and presented in a 3D parameter map using potential relationships. The experimental results of the strongly nonhomogeneous turbulent dynamics shows the different decay of the strongest vortices as a function of the local Richardson number and the interaction mechanisms between inertial and internal waves. The basic Kolmogorov self-similar theory K41&K62 are not applicable as the flow exhibits some clear non-local properties, even not being two-dimensional.

Evolution of tracers at the centre of a density interface

PIV of the interaction of internal Waves and vortices

Turbulent entrainment in jets: large and small scale physics and consequences for LES

Carlos B. da Silva*, Ricardo J. N. dos Reis, Rodrdigo R. Taveira and José Carlos Fernandes Pereira

IDMEC/IST, Mecânica I, 1° andar/LASEF
Universidade Técnica de Lisboa, Av. Rovisco Pais, 1049-001 Lisbon, Portugal
e-mail: Carlos.Silva@ist.utl.pt
Web page: http://www.lasef.ist.utl.pt

ABSTRACT

This work analysis several large and small scale aspects of the turbulent entrainment mechanism that exists in mixing layers, wakes, and jets. The entrainment that takes place across a turbulent/nonturbulent (T/NT) interface that divides the irrotational (nonturbulent - NT) from the turbulent (T) region in these flows. Turbulent entrainment is important to many natural and engineering flows since important exchanges of mass, momentum and passive or active scalar quantities take place across the T/NT interface. It was assumed in the past that the entrainment is mainly driven by "engulfing" motions caused by the large scale flow vortices, but recent experimental and numerical works give more support to the original model of Corrsin and Kistler [1] where the entrainment is primarily associated with small scale ("nibbling") eddy motions (Mathew and Basu [2], Bisset *et al.* [3], Westerweel *et al.* [4]). Recently, using a direct numerical simulation (DNS) of a turbulent plane jet at $Re_\lambda \approx 120$ da Silva and Pereira [5] analyzed the invariants of the velocity-gradient, rate-of-strain, and rate-of-rotation tensors across the T/NT interface in order to characterize several aspects of the small scale dynamics near the T/NT interface. The challenges faced by the subgrid-scale models in this context were analyzed in detail by da Silva [6]. The present work focuses on the dynamics of the kinetic energy near the T/NT interface, and on the role of the intense vorticity structures (IVS), as defined by Jiménez [7], near the jet edge.

REFERENCES

[1] S. Corrsin and A. L. Kistler. Free-stream boundaries of turbulent flows. Technical Report TN-1244, NACA, 1955.

[2] J. Mathew and A. Basu. Some characteristics of entrainment at a cylindrical turbulent boundary. *Phys. Fluids*, 14(7):2065–2072, 2002.

[3] D. K. Bisset, J. C. R. Hunt, and M. M. Rogers. The turbulent/non-turbulent interface bounding a far wake. *J. Fluid Mech.*, 451:383–410, 2002.

[4] J. Westerweel, C. Fukushima, J. M. Pedersen, and J. C. R. Hunt. Mechanics of the turbulent-nonturbulent interface of a jet. *Phys. Review Lett.*, 95:174501, 2005.

[5] C. B. da Silva and J. C. F. Pereira. Invariants of the velocity-gradient, rate-of-strain, and rate-of-rotation tensors across the turbulent/nonturbulent interface in jets. *Phys. Fluids*, **20** 055101, 2008.

[6] C. B. da Silva. The behavior of subgrid-scale models near the turbulent/nonturbulent interface in jets. *Phys. Fluids*, **21**, 081702, 2009.

[7] J. Jimenez, A. Wray, P. Saffman, and R. Rogallo. The structure of intense vorticity in isotropic turbulence. *J. Fluid Mech.*, 255:65–90, 1993.

Vorticity, Kinetic Energy and Momentum Analysis
Of the Collision Zone between a Plane Wall Jet and a Boundary Layer

Jorge M. M. Barata, Ricardo B. F. Nunes, Pedro J.C.T. Santos and André R. R. Silva
Universidade da Beira Interior, Covilhã, 6201-001, Portugal

When a Short/Vertical Take-off and Landing (V/STOL) aircraft is lifting off or landing with zero or small forward momentum, a complex flow can be found near the ground. The lifting jets impinge on the ground and originate wall jets that interact between them forming an upwash or collide with any crosswind present. In this latter case a highly curved flow exists upstream of the impinging stagnation point. This highly curved flow is known as "ground vortex", and has profound influences on the flow development and aircraft operation.

Measurements of this type of flows are very scarce in the literature, and are reported as a secondary flow within the impinging jet flow problem, and are dispersed among many different configurations and operating conditions. The present work is included in a research program dedicated to the identification of the parameters and regimes associated with instabilities, and other secondary effects of this ground vortex flow. A detailed analysis of a ground vortex resulting from the collision between a wall jet and a boundary layer has been performed, and follows the previous study of Barata et al. (2005), which detected a small secondary recirculation zone located upstream the separation point not reported before. To avoid the influence of the impinging region due to the lift jet, a plane turbulent wall jet is produced independently. The wall jet collides with the boundary layer produced by a conventional wind tunnel creating the ground vortex. Laser Doppler measurements are presented for a velocity ratio between boundary layer and wall jet (V_R) of 0.5, and include mean and turbulent velocity characteristics along the two normal directions in the vertical plane of symmetry of the flow.

Vorticity, turbulent kinetic energy, and momentum balances were determined from the measured data in order to understand the complex nature of the flow in the collision zone near the ground wall, which is characterized by up to three well-defined turbulent structures that change their size and shape with time. The experimental results were complemented with transient RANS computations, and three distinct flow patterns were observed for different velocity ratios intervals. Low frequency features were detected by a small hump in the measured power spectra for V_R=0.5. The experimental results were complemented with some preliminary transient RANS computations. These calculations exhibited transient structures for V_R =0.1, 0.125, and 0.15, but for lower or higher values the flow was found to be stationary. The analysis of the transport equations from the measured data revealed important production of turbulent kinetic energy by normal stresses, together with a dominant pressure term in the momentum equations in the collision zone.

The detailed nature of the measurements and the indications collected from the preliminary calculations makes the present experimental data eminently suited for modelling purposes.

Symmetry breaking, intermittent transition and swirl switching in a flow of physiological interest

J.M.M. Sousa

Mechanical Engineering Department, Instituto Superior Técnico, Technical University of Lisbon

Av. Rovisco Pais, 1049-001 Lisboa, Portugal

Time-dependent numerical simulations of a simple flow of physiological interest have been performed for Reynolds numbers in the range 100-400. The present results have demonstrated that the flow reaches asymptotically steady, symmetrical solutions for Reynolds numbers up to 300, whereas a value of 400 for this parameter leads to unsteadiness. The computed flow behavior at this higher Reynolds number has shown to be characterized by an intermittent transition between small-amplitude, irregular oscillations and large-amplitude bursts occurring at a low frequency. In addition, the unsteady flow was asymmetrical and exhibited swirl switching.

DNS SIMULATION OF A TRANSITIONAL LAMINAR SEPARATION BUBBLE ON A FLAT PLATE

C.LAURENT*, I.MARY*, V.GLEIZE*, A.LERAT**, D.ARNAL*.
*: ONERA (France) ; **: SINUMEF (France)

The objective of the current study is to create a numerical data base of a transitional laminar separation bubble flow, in order to improve the understanding of the mechanisms involved and to help the improvement of the RANS turbulence models. In order to provide helpful insights into this complex flow, DNS simulations of a laminar separation bubble on a flat plate with an adverse pressure gradient have been performed. A grid convergence study has been achieved and particular attention has been given to the theoretical validation of the three states encountered by the fluid: laminar, transitional and turbulent.

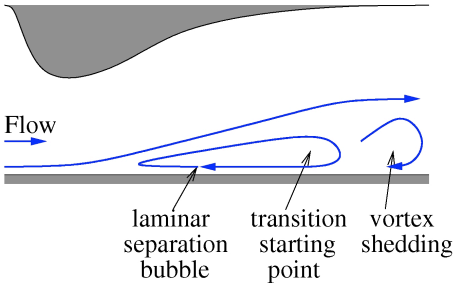

(a) Structure of the flow

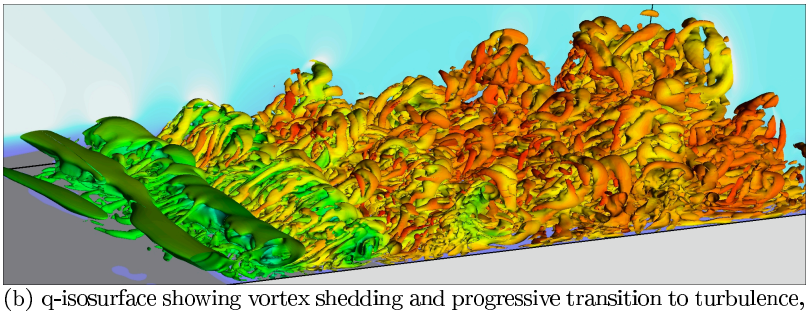

(b) q-isosurface showing vortex shedding and progressive transition to turbulence, colored by density. Background colored by longitudinal speed amplitude.

Introduction

The transitional laminar separation bubble occurring near the leading edge of a profile is a complex flow phenomenon induced by a strong adverse pressure gradient (APG); it is characterised by a recirculation area where transition occurs, and can lead to stall by a sudden drop of lift and increase of the drag coefficents. Hence, the correct simulation of these phenomena is important for the design of many industrial domains, such as helicopter rotor blades or jet engines.

Nowadays, RANS methods give the possibility to calculate flows on complex geometries ; they are widely used to compute stall but often fail to predict correctly its occurence [1], as they are based on assumptions not validated with such complex flow phenomena (transition, APG). The improvement of these methods is essential, which requires a good reference data base. For this purpose, several DNS calculations on grids of different resolutions have been achieved.

DNS Simulations

The choice has been made to study the flow on a flat plate instead of a profile to reduce the complexity of the flow, and allow a better analysis of the physical phenomena involved. The pressure gradients (first negative then positive) are set up to be characteristics of the leading edge of a profile. They are controlled by an upper wall whose distance to the flat plate varies along the flow (see fig. a).

The unit Reynolds number at the boundary layer edge is equal to 8.10^6 and the Mach number to 0.4 after the end of the channel's height variation. The resolution of the finest mesh is characterised by $\Delta y^+ \leq 0.7$, $\Delta z^+ \leq 7$, and by $\Delta x^+ \leq 7$ in the bubble area, then increasing slowly until $\Delta x^+ = 27$.

The laminar part of the flow (before separation) is validated by its good agreement with a boundary layer calculation in terms of skin friction, displacement thickness and shape factor.

The study of the transitional part shows an exponential amplification of the fluctuations with a predominant frequency of fluctuation around $70 - 80\,kHz$. A linear stability calculation confirmed the high amplification of these particular frequencies.

The boundary layer following the reattachment becomes turbulent and the predominance of the particular frequencies slowly disappears. The grid convergence study shows a satisfying convergence of the velocity profiles towards the logarithmic law, without actually reaching it, which is not surprising as the Reynolds based on the boundary layer momentum thickness θ increases up to 1500 only.

A set of statistics is still being computed from the DNS, it includes the calculation of the different terms of the Reynolds tensor transport equation, and will allow a future comparison of these DNS-issued statistics with the terms of the RANS turbulence models.

References

[1] V. Gleize, J. Szydlowski, and M. Costes. Numerical and physical analysis of turbulent viscous flow around a NACA0015 profile at stall. *European Congress on Computational Methods in Applied Sciences and Engineering*, Jyväskylä, Finland, 2004.

Kinetic energy and dissipation profiles calculated from RDT near a turbulent-non-turbulent interface

Miguel A. C. Teixeira[1] and Carlos. B. da Silva[2]

[1]CGUL, IDL, University of Lisbon, Lisbon, Portugal
[2]LASEF, IDMEC/IST, Technical University of Lisbon, Lisbon, Portugal

We use rapid-distortion theory (RDT) to compute turbulence statistics near an interface separating a zone in a fluid that is quiescent from a zone where homogeneous and isotropic turbulence is assumed to exist. This idealized situation roughly represents the edge of a turbulence zone (e.g., a jet), where turbulent entrainment takes place. Since RDT is linear, the interface is treated as essentially flat, and nonlinear interactions among the turbulent eddies are neglected. Thus, inside the turbulence there are no pressure fluctuations, and there is no mean flow into the turbulence (corresponding to the entrainment velocity). However, both the inviscid dynamics associated with continuity of the normal velocity and of pressure at the interface, and the growth of viscous boundary layers, are explicitly taken into account. This can be shown to be a good approximation for early times after a hypothetical sudden insertion of the interface. The present study addresses the small-scale processes ('nibbling') which have been shown to be responsible for the entrainment that takes place in the vicinity of the turbulent-non turbulent interface. A characterization of these processes is useful for the future development of subgrid-scale parametrization schemes for use in LES.

Inviscid results show that both the velocity variances tangential to the interface, and the kinetic energy, as well as the kinetic energy dissipation, display a discontinuity at the interface, with well defined values, not dependent on the detailed form of the assumed energy spectrum in the turbulent zone, at the inner and outer limiting regions approaching the interface. These discontinuities result directly from the boundary conditions imposed at the interface. As one moves away from the interface into the non-turbulent zone, the kinetic energy and dissipation are found to decay as z^{-4} and z^{-6}, respectively (where z is distance from the interface), in accordance with classical estimates by previous authors [1].

Viscous boundary layers at each side of the interface must be introduced in order to satisfy the continuity of tangential velocity components, and of the viscous stresses. When these effects are taken into account, the problem becomes unsteady, with the thickness of the boundary layers increasing with time up to the point where the assumed approximations break down.

Profiles for the velocity variances, the kinetic energy and the dissipation then vary smoothly, and are compared with direct numerical simulation results for similar quantities [2], adequately conditionally averaged so as to account for the complicated topology of the interface.

[1] O. M. Phillips. The irrotational motion outside a free turbulent boundary. *Proc. Camb. Phil. Soc.*, 51:220, (1955).
[2] C. B. da Silva and J. C. F. Pereira. Invariants of the velocity-gradient, rate-of-strain, and rate-of-rotation tensors across the turbulent/nonturbulent interface in jets. *Phys. Fluids*, 20:055101, (2008).

Vortices and Spiral Features in the Ocean Surface

A. Matulka (1,2)P. Fraunie(1),P. Forget(1) , J. M. Redondo2 , A. Platonov2
M. Diez2, C. Mosso2, R. Castilla3 and E. Sekula2

1Laboratoire de Sondages Electromagnétiques de l'Environnement Terrestre
Université Sud Toulon Var - CNRS, BP 20132, 83957 La Garde, France
2Dept. de Fisica Aplicada.3(Mecanica fluidos)Univ. Politecnica de Catalunya,
B5 Campus Nord UPC , Barcelona 08034, Spain

E-mail: anna.margarita.matulka@upc.edu, philippe.fraunie@lseet.univ-tl.fr,
redondo@fa.upc.edu

The advances in radar sensors may be applied to study the flow in the region of fresh water influence (ROFI) region of the ocean. The Synthetic Aperture Radar (SAR) is a useful tool that may be used to study both marine water dynamics and its pollution. Oil spills and natural slicks may be detected and processed with advanced computer techniques to reveal vortex dynamics and turbulence spectral characteristics of the complex eddy and current interaction in the ocean surface. In the framework o the European Union contract Clean Seas, more than 600 SAR images of the North-west Mediterranean Sea area taken between December 1996 and December 2004 were analyzed. A distribution of eddies were detected under certain conditions and we analyzed statistically the appearance, size, gire, elongation and position of vortices and vortex pairs in the test area. It is shown that the maximum size of the eddies detected near the coast is limited by the Rossby deformation radius and that there is a decrease in size in the coastal waters in the direction of the Liguro-Provenzal current with the largest eddies occurring near the cape of Rosas. The role of submarine canyons in the vortex generation is indicated by the asymmetry of their distribution with respect to the thalwegs. It is demonstrated that useful information of a geometrical nature obtained by SAR satellite images may be used to estimate relevant dynamical parameters of coastal flows. In this context, the use of multifractal and spectral measures are useful to predict dispersion in different topological flow regions with the help of SpillSim, a dedicated Kinematic Simulation program.

[1]Gade, M., and J. M. Redondo (1999) 'Marine pollution in European coastal waters monitored by the ERS-2 SAR: a comprehensive statistical analysis". IGARSS 99. Hamburg. v. III, 1637-1639., pp. 308-312.
[2]Jolly G. W., A. Mangin, F. Cauneau, M. Calatuyud, V. Barale, H. M. Snaith, O.Rud, M. Ishii, M. Gade, J. M. Redondo, A. Platonov (2000). The Clean Seas Project Final Report (ENV4-CT96-0334). Ed. DG XII/D, Brusselas.

[3]R. Castilla, Redondo, J. M., A. K. Platonov. (2003). SpillSim Manual Version 1.4. DFA/UPC. Barcelona, Spain. pp. 1-33.
[4] Reffray G., Fraunié P. and P. Marsaleix 2004. Secondary flows induced by wind forcing in the Rhone region of freshwater influence. Ocean Dynamics, 54: 179–196.

[5] Hu, Z.H., Doglioli, A.M., Petrenko, A.A., Marsaleix, P., Dekeyser, I. (2009), Numerical simulations of eddies in the Gulf of Lion. Ocean Model., Vol. 28/4, pp. 203-208, doi : 10.1016/j.ocemod.2009.02.004
[6] Bezerra M.O., Diez M., Medeiros C. Rodriguez A., Bahia E., Sanchez Arcilla A and Redondo J.M. (1998) "Study on the influence of waves on coastal diffusion using image analysis'. Applied Scientific Research, 59,127-142.
[7] Bunimovich L.A., Ostrovsky A.G., Umatani S. (1993). Observations of the fractal properties of the Japan Sea surface temperature patterns. Int. J. Remote Sensing, v. 14, No 11, pp. 2185-2201.
[8]Carrillo, A. Sanchez, M.A. Platonov, A.Redondo, J.M., (2001). Coastal and Interfacial Mixing. Laboratory Experiments and Satellite Observations. Physics and Chemistry of the Earth, v. B, 26/4. pp. 305-311.
[9]Redondo J.M. (1996) "Vertical microstructure and mixing in stratified flows". Advances in Turbulence VI. Eds. S. Gavrilakis el al. 605-608.

Estimation of turbulent convection velocities and corrections to Taylor's approximation

J. C. del Álamo [2,1] and J. Jiménez [1,3]

[1] School of Aeronautics, U. Politécnica Madrid. 28040 Madrid. Spain
[2] MAE Department, U. California San Diego, La Jolla, CA 92093, USA.
[3] Centre for Turbulence Res., Stanford U., Stanford, CA 94305, USA

A new method is introduced for estimating the convection velocity of individual modes in turbulent shear flows, based on minimizing the magnitude of the advective derivatives. In contrast to most previous ones, space-time information is not needed. Spectral information is only required in the direction, time or space, in which a modal decomposition is desired, while in the other direction it only uses local derivatives. If no spectral information is desired, the method provides a natural definition for the average convection velocity, and an estimation of the accuracy of the frozen-turbulence approximation. The new method is validated against classical ones, and applied to existing turbulent channel simulations to show that small scales travel with the local mean velocity, while large "global" modes travel with a uniform speed proportional to the bulk velocity. A semiempirical fit to the computed convection velocities is given that represents well the data throughout the Reynolds number range of the simulations, and which can be used to estimate the effect of applying the standard Taylor's approximation. Not only are the large scales displaced to shorter apparent wavelengths, but the shape of the spectrum is changed, giving rise to spurious spectral peaks similar to those that have been observed in experiments.

When this is applied to simulation data, for which the true two-dimensional spatial spectra are known, it is found that some of the large-scale spectral peaks reported in experiments are probably artifacts of the temporal approximation, and that the true structure of wall-bounded flows is probably much closer to the classical k^{-1} behaviour suggested by Townsend.

Mixing Through Stable and Unstable density interfaces

P. Lopez Gzlez-Nieto(1,2)J.L. Cano(1), D.Hernandez (3) , J. M. Redondo (2,3) , and P. Furmanek 3

1 Facultad de Fisicas & 2 Instituto Pluridisciplinar. Universidad Complutense de Madrid, C. Universitaria. Madrid, Spain
3 Dept. de Fisica Aplicada. Univ. Politecnica de Catalunya, B5 Campus Nord UPC , Barcelona 08034, Spain

Geometrical Lagrangian (PIV)and Eulerian point measurements of density and velocity have been used to compare entrainment and mixing efficiencies across density interfaces both in stable and unstable situations. Rayleigh-Taylor driven flows exhibit the highest efficiencies, but these are very dependent on the initial conditions of the overturning flow. On the other hand, stable interfaces have lower mixing efficiencies that depend strongly on the parameter range of the external stirring. The local Richardson number, the Schmidt number and the Reynolds number, determine the probability distribution of internal Waves, Holmboe waves and Kelvin-Helmholtz billows, when the buoyancy acts as an energy sink.

[1]Redondo J.M. and Cantalapiedra I.R. (1993) "Mixing in horizontally heterogeneous flows", Applied Scientific Research, 51, 217-222.
[2] Richardson L. F., Proc. R. Soc. London, Ser A, 110 (1926) 709.
[3] Kolmogorov A. N., C. R. Acad. Sci. USSR, 30 (1941) 301.
[4] Kolmogorov A. N., J. Fluid Mech., 13 (1962) 82.
[5] Kraichnan R., Phys. Fluids, 10 (1967) 1417.
[6] Linden P. F., Boubnov B. M. and Dalziel S. B., J. Fluid Mech., 298 (1996) 81.
[7] Carrillo A. A., Sanchez M. A., Platonov A. and Redondo J. M., Phys. Chem. Earth B, 26 (2001) 305.
[8] Chen X. and Allen S. E., J. Geophys. Res., 101 (1996) 18043.
[9] Mahjoub O. B., Redondo J. M. and Babiano A., J. Flow Turbul. Combust., 59 (2000) 299.
[10] Redondo J. M. and Linden P. F., Geometrical Observations of Turbulent Interfaces:The Mathematics of Deforming Surfaces (IMA 56, Clarendon Press, Oxford) 1996. 221-248.

NUMERICAL SIMULATION OF THE TURBULENT FLOW IN THE SUCTION CHAMBER OF AN EXTERNAL GEAR PUMP INCLUDING CAVITATION EFFECTS

DAVID DEL CAMPO, ROBERTO CASTILLA AND ESTEVE CODINA
SCHOOL OF MECHANICAL AND AERONAUTICAL ENGINEERING, TECHNICAL UNIVERSITY OF CATALONIA, TERRASSA, SPAIN

The flow in the suction chamber of an external gear pump is numerically analysed at different rotational speeds using a commercial computational fluid dynamics (CFD) solver, FLUENT® 12.0.16. A 2D model with a total contact ratio of 1 (only one contact point in the gearing line) is used. The evolution of the boundaries of the domain is very complex, and an Arbitrary Lagrangian-Eulerian (ALE) formulation is used with mesh deformation and local remeshing. Nevertheless, in order to avoid skewed meshes, a mesh replacement strategy is adopted. This technique consists of interpolating the solution over a new mesh each time 1/10 of a gearing cycle is completed.

Standard $k-\varepsilon$ turbulence model has been used as it showed to be a good approach in previous studies. All equations are solved using a second-order upwind sheme with a node-based calculation of the gradients. In order to model the pressure terms, the body-force-weighted scheme, which computes the face pressure by assuming that the normal gradient of the difference between pressure and body forces is constant, is used.

For rotational speeds above 300 rpm cavitation effects appear, therefore reducing the volumetric effectiveness of the pump. In order to take this into account, a multiphase mixture model (single-phase approach) with no slip velocity has been adopted. To model the phase transfer mechanism, the relatively new Schnerr and Sauer cavitation model (based on the Rayleigh-Plesset equation) has been used. This model accounts for all first-order effects (i.e., phase change, bubble dynamics, turbulent pressure fluctuations, and noncondensable gases) and has the capability to account for the compressibility of both liquid and gas phases.

The contact point was initially modeled as a tiny wall linking both gears by the same two nodes, therefore moving and deforming with the mesh. To avoid big separations from the theoretical position of the contact point, the wall position was corrected after each mesh replacement. This strategy, which showed to be valid without multiphase models, results in a strong mesh dependance of the solution when cavitation is present. Therefore, the strategy that is being tested consists of modeling the exact theoretical position of the contact point in each time step by changing the characteristic of the zone that separates the two solids from "fluid" to "solid" when the separation becomes smaller than an small defined value, and back from "solid" to "fluid" when it becommes bigger.

The simulations are currently running.